DOI: 10.1002/ejoc.200600318

Enhanced Electron Transfer Rate in a Rigid Ferrocene–Fulleropyrrolidine Dyad

Francesco Caporossi,[a] Barbara Floris,[a] Pierluca Galloni,*[a] Emanuela Gatto,*[a] and Mariano Venanzi[a]

Keywords: Ferrocene / Fullerene / Electron transfer / Donor-acceptor system / Dyads

A rigid ferrocene–fullerene dyad was obtained from fullerene (C_{60}), *N*-methylglycine and 1,1′-(α-oxotrimethylene)ferrocene. The frozen geometry resulted in an enhanced electron transfer rate from ferrocene to fullerene moieties, when compared with conformationally flexible *N*-methyl-2-ferrocenylfulleropyrrolidine.

Introduction

Electron transfer (ET) reactions are an important topic of current research, being related both to understanding of natural systems[1] and to development of new electronic devices.[2] The strategy to achieve efficient ET and long-lived charge transfer (CT) states generally requires complex multi-component systems.[3] Alternatively, small systems called "compact dyads", capable of fast charge separation and slow charge recombination, have been largely investigated.[4]

Ferrocene (Fc)–fullerene (C_{60}) dyads represent a good model to investigate electron transfer processes. Generally, these two entities are covalently linked to form fulleropyrrolidine (C_{60}pyrr) derivatives,[5] or are involved in supramolecular systems by π–π interaction.[6] A few examples have been reported so far, where the two components are linked by cumulene spacers,[7] acetylenic linkages,[8] or fused and substituted cyclopropane (by Bingel reaction).[9] An example of a compact dyad was also reported, with ferrocene directly linked to azafullerene.[10] Photophysical studies on Fc–C_{60} dyads have shown that ET occurs from Fc to the C_{60} singlet excited state, with efficiencies depending on the geometry and the nature of the spacer.[5,8] The experimentally observed quenching of fullerene emission has been therefore attributed to Fc→C_{60}* ET.[5,8]

Since the photophysical properties of *N*-methyl-2-ferrocenyl-3,4-fulleropyrrolidine are well established and the compound is known to undergo electron transfer, we wanted to investigate how it was affected by introducing conformational freezing. Thus, a new compact dyad based on the Fc and C_{60} molecular components was synthesized with the aim to obtain a rigid Fc–C_{60}pyrr system.

Results and Discussion

We applied the Maggini–Prato–Scorrano reaction,[5] formerly developed for aldheydes and simple aliphatic ketones, to a ferrocenyl ketone to obtain the target dyad **d1** shown in Scheme 1. Dyad **d1** was prepared in 26% yield by heating fullerene (C_{60}), *N*-methylglycine and 1,1′-(α-oxotrimethylene)ferrocene in toluene (Scheme 2).

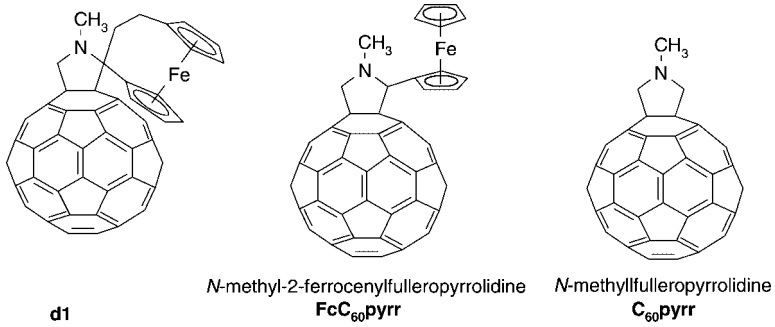

d1 — *N*-methyl-2-ferrocenylfulleropyrrolidine **FcC_{60}pyrr** — *N*-methylfulleropyrrolidine **C_{60}pyrr**

Scheme 1. Molecular structure of the rigid (**d1**) and flexible (FcC_{60}pyrr) ferrocene–fullerene dyads. *N*-Methyl-3,4-fulleropyrrolidine (C_{60}pyrr) is used as the reference compound for photophysical studies.

[a] Università di Roma "Tor Vergata", Dipartimento di Scienze e Tecnologie Chimiche,
Via della Ricerca Scientifica, 00133 Roma, Italy
Fax: +39-06-72594-328
E-mail: galloni@scienze.uniroma2.it
emanuela.gatto@uniroma2.it

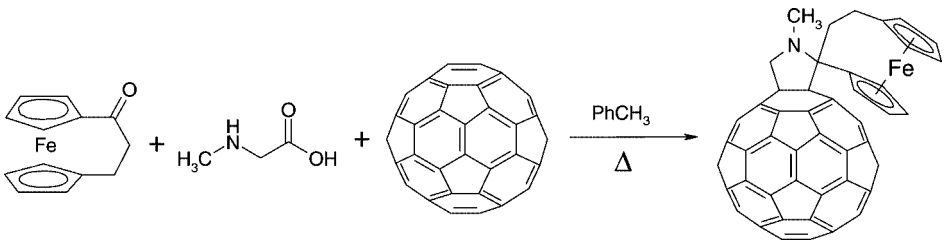

Scheme 2. Synthesis of dyad **d1**.

The molecular structure and identity of **d1** was confirmed by NMR, MALDI and ESI mass spectrometry; no crystals suitable for X-ray analysis could be obtained. Dyad **d1** was also characterized by UV/Vis absorption, cyclic voltammetry (CV), and theoretical calculations as well. The ^{1}H NMR spectrum, shown in Figure 1, reveals that each proton in **d1** gives rise to a well-resolved signal, including those that are generally found as magnetically equivalent, such as methylene groups or α- and β-protons of the substituted cyclopentadienyl ring. This result is rather unusual and is very likely due to the conformational rigidity of **d1**; a precedent can be found in a C_{60}–Fc *ansa* derivative obtained from 1,1′-bis(diazoacetyl)ferrocene and fullerene.[11] In the flexible compound FcC_{60}pyrr, the α- and β-protons are magnetically equivalent, as is typical of substituted ferrocenes.[12]

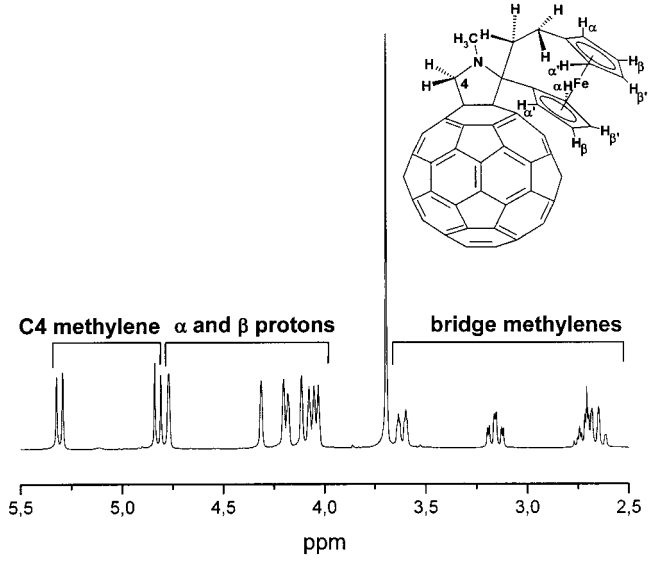

Figure 1. ^{1}H NMR spectrum of dyad **d1**.

With the aim of investigating the effects of the **d1** rigid structure, its photophysical properties were studied in comparison with those of the well-known *N*-methyl-2-ferrocenylfulleropyrrolidine (FcC_{60}pyrr).[5,12]

The UV/Vis spectra of **d1** and FcC_{60}pyrr are almost completely superimposable (Figure 2), thus indicating the absence of new absorption features ascribable to charge transfer interactions in the Fc–C_{60} ground state.

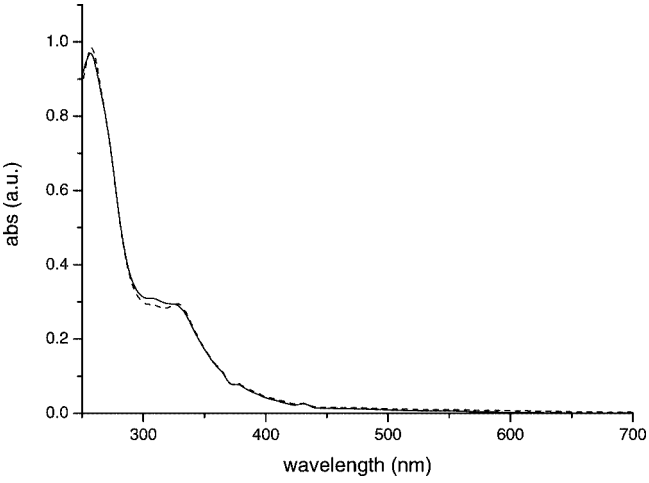

Figure 2. UV/Vis spectra of dyad **d1** (solid line) and *N*-methyl-2-ferrocenylfulleropyrrolidine (dotted line) in $CHCl_3$. Molar concentration of both solutions: $7.0 \cdot 10^{-6}$ M.

Cyclic voltammetry (CV) measurements of both **d1** and FcC_{60}pyrr show an oxidation peak at around 0.49 V vs. SCE (Fc oxidation) and a reduction peak at –0.59 V vs. SCE (C_{60}pyrr reduction). These results suggest that the HOMO and LUMO of both compounds are localized on the ferrocene and fullerene moieties, respectively. Theoretical calculations were carried out to reinforce this conclusion. Geometry optimization (Gaussian 03, B3LYP3-21g* basis set) confirmed that **d1** adopted a conformationally rigid structure (shown from two different perspectives in Figure 3), as suggested by its peculiar ^{1}H NMR spectrum.

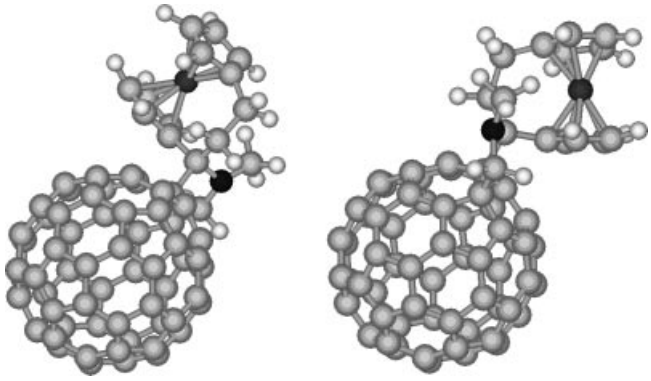

Figure 3. Different views of the optimized geometry of dyad **d1** (ball-and-stick representation).

In agreement with CV experiments, the **d1** HOMO and LUMO are centered on the Fc and C_{60} groups, respectively. All these findings point to the conclusion that ground state interactions between the Fc and C_{60} moieties in **d1** are weak, and that the two molecular components can be considered as electronically independent.

Photophysical experiments were performed to analyze the effect of the **d1** frozen geometry on excited state interactions. As stated above, quenching of the C_{60} emission in Fc–C_{60}pyrr dyads takes place by ET from Fc to the singlet excited state of fulleropyrrolidine.[13] The pathway of this ET process has been attributed to a through-space or a through-bond mechanism, depending on the nature of the linkage. In the case of FcC_{60}pyrr, a through-bond pathway has been shown to predominate due to the short spacer separating the donor and acceptor pair.[5] An energy transfer process can be ruled out because the emission spectrum of *N*-methylfulleropyrrolidine is not superimposable on the absorption spectrum of the ferrocene moiety.

Steady-state and time-resolved fluorescence experiments were carried out on **d1**, FcC_{60}pyrr and *N*-methylfulleropyrrolidine (C_{60}pyrr). The latter was used as the reference compound for photophysical studies. The emission spectra of the investigated compounds are shown in Figure 4.

As can be seen from Figure 4, C_{60}pyrr displays the strongest fluorescence intensity, while the emissions of both **d1** and FcC_{60}pyrr are extensively quenched. It is interesting to compare the ET rates of **d1** and FcC_{60}pyrr, as obtained from their fluorescence quantum yields (Φ) and the fluorescence quantum yield (Φ_0) and lifetime (τ_0) of the C_{60}pyrr reference compound, i.e., $k_{ET} = [(\Phi_0/\Phi) - 1]/\tau_0$. From the data reported in Table 1, it appears that the **d1** ET rate constant is three times faster than that of FcC_{60}pyrr. The more efficient electron transfer of **d1** can be explained as a consequence of the two Fc–C_{60} linkages opening multiple through-bond ET pathways. However, effects of the rigid **d1** structure on the nuclear reorganization energy (λ) of the ET reaction should be also taken into account to quantitatively explain the differences in the ET rate constants of **d1** and Fc–C_{60}pyrr.

To further investigate the nature of the Fc–C_{60}pyrr interaction, transient absorption experiments between 380 and 600 nm with nanosecond time resolution were carried out. For all the examined compounds, transient absorption bands ascribable to the fullerene triplet–triplet absorption were observed, with a maximum at 420 nm. In the case of FcC_{60}pyrr, signals ascribable to transient radical species generated by the ET process in the ns–μs time range were not detected. Guldi et al. suggested that in the Fc–C_{60} compact dyad, ET takes place by a through-bond mechanism followed by a fast, subnanosecond charge recombination across the short bridge, thus preventing the observation of radical species even in a polar solvent like benzonitrile.[5] Transient absorption time decays at λ = 400 nm of C_{60}pyrr

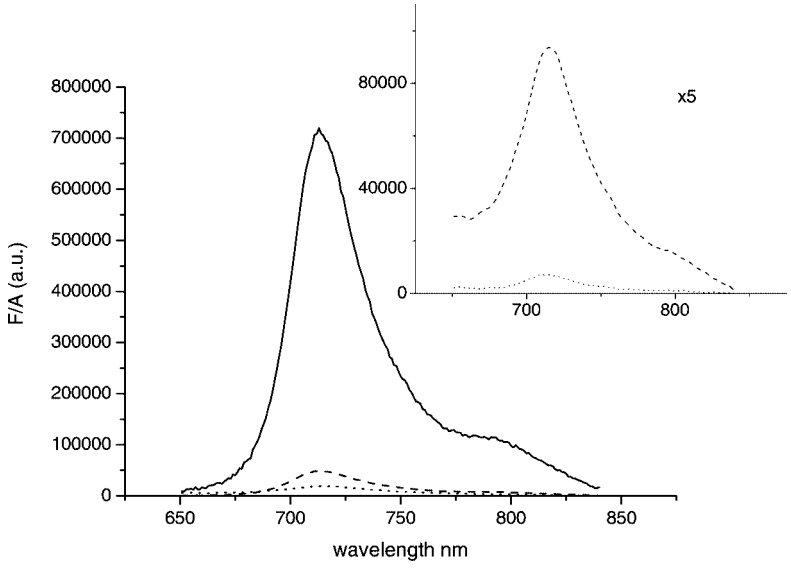

Figure 4. Steady-state fluorescence spectra of C_{60}pyrr (solid line), FcC_{60}pyrr (dotted line) and **d1** (dashed line) in benzonitrile. Inset: Fluorescence spectra of FcC_{60}Pyrr and **d1** magnified by a factor of 5 for comparison; λ_{exc} = 332 nm.

Table 1. Quantum yields and steady-state quenching efficiencies of *N*-methyl-3,4-fulleropyrrolidine, *N*-methyl-2-ferrocenyl-3,4-fulleropyrrolidine, and dyad **d1**.

	$10^4\ \Phi$	E	$10^{-9}\ k_{ET}$ [s^{-1}]
N-Methyl-3,4-fulleropyrrolidine[a]	2.57 ± 0.03		
N-Methyl-2-ferrocenyl-3,4-fulleropyrrolidine	0.10 ± 0.01	0.96	17.6
Dyad **d1**	0.04 ± 0.01	0.99	45.2

[a] τ_0 = 1.4 ns.

Table 2. Triplet state amplitude and rate constants from transient absorption experiments in benzonitrile.

	$\Delta A(0)/A$(355 nm)	10^{-5} k_T [s^{-1}]	E_T
N-Methyl-3,4-fulleropyrrolidine	0.052 ± 0.003	1.03 ± 0.02	
N-Methyl-2-ferrocenyl-3,4-fulleropyrrolidine	0.006 ± 0.001	1.8 ± 0.6	0.42
Dyad **d1**	0.002 ± 0.001	2.2 ± 0.5	0.52

and FeC_{60}pyrr in degassed benzonitrile are shown in Figure 5, while the normalized differential absorptions at t = 0, $\Delta A(0)/A$(355 nm), and the triplet state depletion rate constants, k_T, are reported in Table 2.

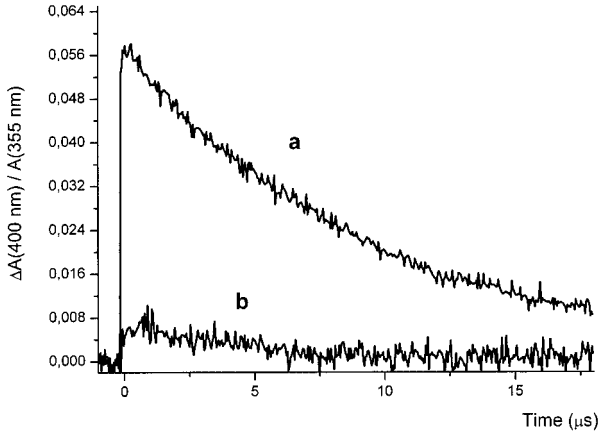

Figure 5. Transient absorption decays (λ = 400 nm) of C_{60}pyrr (a) and FeC_{60}pyrr (b) in benzonitrile.

The $\Delta A(0)/A$ values, being proportional to the triplet state population, follow the opposite trend of the singlet state quenching efficiency because of the competition between electron transfer and singlet-triplet intersystem crossing (ISC). This result confirms that the intramolecular reductive quenching by Fc takes place from the C_{60} excited singlet state. As far as the k_T rate constants are concerned, they are directly related to the photophysical processes depleting the triplet excited state population. The nanosecond transient absorption decay of **d1** reveals interesting differences with respect to those of C_{60}pyrr and FeC_{60}pyrr. The **d1** transient spectrum shows the typical peak at 400 nm,[5] and a characteristic biexponential time decay behaviour (Figure 6), with a fast time component ($k_1 = 4.3 \cdot 10^7$ s^{-1}) and a slower decay ($k_2 = 2.18 \cdot 10^5$ s^{-1}), the latter ascribable to the triplet state decay.

A fast decay at 400 nm in an Fc–C_{60} dyad has been observed and attributed to the C_{60} radical anion.[5] The observation of a long-lived charge transfer state in the nanosecond time regime implies that, following a fast forward ET event, a slow charge recombination necessarily takes place. By comparison with the photophysical behaviour of FeC_{60}pyrr, this effect can be attributed to the rigid molecular architecture of **d1**. A tentative explanation might be that, within the classical Marcus picture of ET reactions, while forward ET often takes place in the Marcus normal region, $|\Delta G°| < \lambda$, charge recombination often occurs in the inverted region, i.e. $|\Delta G°| > \lambda$.[14] In this case, lowering the

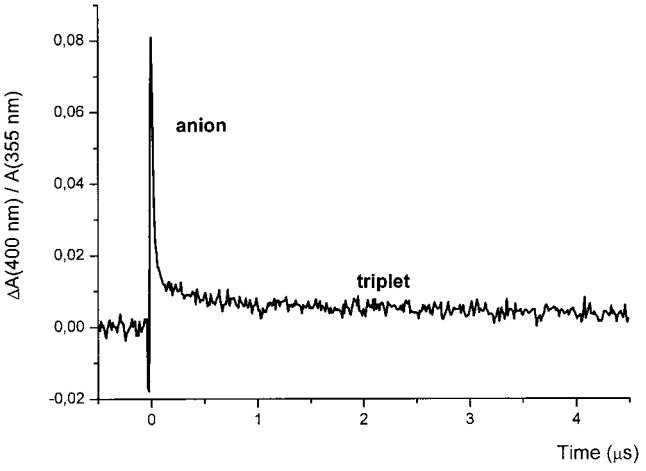

Figure 6. Transient absorption decays (λ = 400 nm) of dyad **d1** in benzonitrile.

nuclear reorganization energy promotes rapid ET in the normal region, but leads to decreased rates in the inverted regime.

Conclusions

With this peculiar ferrocene–fullerene dyad, the lifetime of electron transfer was increased to the nanosecond scale. This investigation demonstrated the possibility of tuning the ET rate and the lifetime of the ensuing charge-separated state by modulating the rigidity of the spacer bridging a compact dyad.

Experimental Section

General: NMR spectra were recorded with a Bruker AMX 400 spectrometer in $CDCl_3$. Solvent residual signals were used as reference (δ =7.23 ppm). Electrochemical experiments were performed with an AUTOLAB PGSTAT10 instrument with PGSTAT-12 using GPES software. A three-electrode system was used, consisting of a platinum (Pt) working electrode, a platinum (Pt) auxiliary electrode, and an SCE reference electrode separated from the test solution by a glass frit. Benzonitrile containing 0.1 M tetrabutylammonium perchlorate was the solvent. Electronic absorption spectra were recorded with a Varian Cary 100 scan UV/Vis spectrophotometer, using 1 cm silica cells and $CHCl_3$ as the solvent. Photophysical experiments were performed in benzonitrile solution. Steady-state emission spectra were obtained with a SPEX 1681 Fluorolog spectrofluorometer equipped with two double monochromators (excitation and emission) and were corrected for the photomultiplier response. Fluorescence time-resolved experiments were carried out with an Edinburgh Instruments LifeSpec-ps.

Nanosecond transient absorption measurements were performed using an Applied Photophysics LKS.60 apparatus equipped with a laser Quantel BrillantB Nd:YAG Q-switched laser (France) operating at 355 nm. GC analyses were performed with a Varian 3900 instrument equipped with SPD5 capillary column, FID detector and N_2 as carrier gas. GC/MS measurements were performed with a GC/MS Shimadzu CP 6000 equipped with an SPD5 capillary column. HPLC analyses were performed with a SHIMADZU LC-10AD, equipped with a "diode array" SPD-M10A detector, and an SiO_2 column SUPELCO 5 μm 25×0.46 cm, using toluene/hexane (1:1, v/v) as eluent. MALDI mass spectra were performed with a Bruker–Franzen Analytik Reflex time-of-flight instrument (Germany) equipped with a SCOUT ion source using 2,5-dihydroxybenzoic acid (DHB) as the matrix (10 mg/mL in acetone). ESI mass spectra were performed with a Finnigan TSQ 7000 instrument in CH_3CN or CH_3CN/CH_2Cl_2 solution. When necessary, solvents were purified using standard procedures.[15] Toluene was obtained by distillation from Na under N_2. Benzonitrile suitable for electrochemical and photophysical experiments was obtained by distillation from P_2O_5 under N_2. 1,1′-(α-Oxotrimethylene)ferrocene was synthesized in 37% yield, according to a literature procedure[16] by the intramolecular Friedel–Crafts reaction of 3-ferrocenylpropanoic acid with trifluoroacetic anhydride; it was recrystallized from hexane and characterized by GC/MS and NMR spectroscopy.

Synthesis of Dyads: Equivalent amounts (0.1 mmol) of the ferrocenyl derivative and fullerene (C_{60}), and 10 equiv. of sarcosine were refluxed in toluene (150 mL) for 5–26 h. The dyads were purified by column chromatography [silica gel; eluting with toluene/hexane (1:1, v/v) to recover unreacted fullerene, and then with toluene to elute the dyad]. The purity was checked by HPLC (SiO_2 column; 1:1 toluene/hexane). *N*-Methyl-2-ferrocenylfulleropyrrolidine was synthesized according to a literature procedure,[5] and exhibited UV/Vis, CV, NMR and mass spectra in agreement with reported data. Dyad **d1** was synthesized both under classical conditions and using an inert gas and a dry solvent. In both cases, the yield was around 28%, but the use of inert conditions resulted in a shortened reaction time (5 h instead of 26 h). Mass spectra were obtained both with MALDI and ESI techniques (m/z = 988 [M + H$^+$]). The ^{1}H NMR spectrum in $CDCl_3$ is shown in Figure 1.

Computational Protocols: Programs used in the computational investigation were Gaussian 03, revision B.01 and GaussView from Gaussian, Inc.[17]

Acknowledgments

We acknowledge Università di Roma "Tor Vergata" for financial support and Dr. Roberta Seraglia (CNR, Padova) for mass spectra.

[1] See, for example: a) W. Zinth, J. Wachtveitl, *ChemPhysChem* **2005**, *6*, 871–880; b) S. L. Gould, G. Kodis, R. E. Palacios, L. de la Garza, A. Brune, D. Gust, T. A. Moore, A. L. Moore, *J. Phys. Chem. B* **2004**, *108*, 10566–10580; c) P. A. Liddell, G. Kodis, L. de la Garza, A. L. Moore, T. A. Moore, D. Gust, *J. Phys. Chem. B* **2004**, *108*, 10256–10265.
[2] See, for example: A. Cravino, N. S. Sariciftci, *J. Mater. Chem.* **2002**, *12*, 1931–1943.
[3] See, for example: a) D. M. Guldi, H. Imahori, K. Tamaki, Y. Kashiwagi, H. Yamada, Y. Sakata, S. Fukuzumi, *J. Phys. Chem. A* **2004**, *108*, 541–548; b) H. Imahori, D. M. Guldi, K. Tamaki, Y. Yoshida, C. Luo, Y. Sakata, S. Fukuzumi, *J. Am. Chem. Soc.* **2001**, *123*, 6617–6628.
[4] J. Verhoeven, H. J. van Ramesdonk, M. M. Groeneveld, A. C. Benniston, A. Harriman, *ChemPhysChem* **2005**, *6*, 2251–2260 and references cited therein.
[5] D. M. Guldi, M. Maggini, G. Scorrano, M. Prato, *J. Am. Chem. Soc.* **1997**, *119*, 974–980.
[6] A. Arrais, E. Diana, R. Gobetto, M. Milanesio, D. Viterbo, P. L. Stanghellini, *Eur. J. Inorg. Chem.* **2003**, 1186–1192.
[7] B. Bildstein, M. Schweiger, H. Angleitner, H. Kopacka, K. Wurst, K.-H. Ongania, M. Fontani, P. Zanello, *Organometallics* **1999**, *18*, 4286–4295.
[8] M. Fujitsuka, N. Tsuboya, R. Hamasaki, M. Ito, S. Onodera, O. Ito, Y. Yamamoto, *J. Phys. Chem. A* **2003**, *107*, 1452–1458.
[9] a) K.-Y. Kay, L. H. Kim, I. C. Oh, *Tetrahedron Lett.* **2000**, *41*, 1397–1400; b) B. Floris, P. Galloni, R. Seraglia, P. Tagliatesta, *J. Organomet. Chem.* **2003**, *679*, 202–207.
[10] F. Hauke, A. Hirsch, S.-G. Liu, L. Echegoyen, A. Swartz, C. Luo, D. M. Guldi, *ChemPhysChem* **2002**, *3*, 195–205.
[11] V. I. Sokolov, T. V. Potolokova, M. N. Nefedova, A. S. Peregudov, *Russ. Chem. Bull., Int. Ed.* **2003**, *52*, 1452–1453.
[12] M. Prato, M. Maggini, C. Giacometti, G. Scorrano, G. Sandonà, G. Farnia, *Tetrahedron* **1996**, *52*, 5221–5234.
[13] T. Hasobe, H. Imahori, H. Yamada, T. Sato, K. Ohkubo, S. Fukuzumi, *Nano Lett.* **2003**, *3*, 409–412.
[14] R. A. Marcus, N. Sutin, *Biochim. Biophys. Acta* **1985**, *811*, 265–322.
[15] D. D. Perrin, W. L. F. Armarego, *Purification of Laboratory Chemicals*, 3rd ed., Pergamon Press, Oxford, **1988**.
[16] K. L. Rinehart Jr, R. J. Curby Jr, D. H. Gustafson, K. G. Harrison, R. E. Bozak, D. E. Bublitz, *J. Am. Chem. Soc.* **1962**, *84*, 3263–3269.
[17] M. J. Frisch, G. W. Trucks, H. B. Schlegel, G. E. Scuseria, M. A. Robb, J. R. Cheeseman, J. A. Montgomery Jr, T. Vreven, K. N. Kudin, J. C. Burant, J. M. Millam, S. S. Iyengar, J. Tomasi, V. Barone, B. Mennucci, M. Cossi, G. Scalmani, N. Rega, G. A. Petersson, H. Nakatsuji, M. Hada, M. Ehara, K. Toyota, R. Fukuda, J. Hasegawa, M. Ishida, T. Nakajima, Y. Honda, O. Kitao, H. Nakai, M. Klene, X. Li, J. E. Knox, H. P. Hratchian, J. B. Cross, C. Adamo, J. Jaramillo, R. Gomperts, R. E. Stratmann, O. Yazyev, A. J. Austin, R. Cammi, C. Pomelli, J. W. Ochterski, P. Y. Ayala, K. Morokuma, G. A. Voth, P. Salvador, J. J. Dannenberg, V. G. Zakrzewski, S. Dapprich, A. D. Daniels, M. C. Strain, O. Farkas, D. K. Malick, A. D. Rabuck, K. Raghavachari, J. B. Foresman, J. V. Ortiz, Q. Cui, A. G. Baboul, S. Clifford, J. Cioslowski, B. B. Stefanov, G. Liu, A. Liashenko, P. Piskorz, I. Komaromi, R. L. Martin, D. J. Fox, T. Keith, M. A. Al-Laham, C. Y. Peng, A. Nanayakkara, M. Challacombe, P. M. W. Gill, B. Johnson, W. Chen, M. W. Wong, C. Gonzalez, J. A. Pople, *Gaussian 03*, revision B.01, Gaussian, Inc., Pittsburgh, PA, **2003**.

Received: April 11, 2006
Published Online: July 28, 2006

